Heliyon 5 (2019) e02669

Contents lists available at ScienceDirect

Heliyon

journal homepage: www.heliyon.com

Research article

Daidzein cocrystals: An opportunity to improve its biopharmaceutical parameters

Yashika Bhalla, Kunal Chadha, Renu Chadha *, Maninder Karan

University Institute of Pharmaceutical Sciences, Panjab University, Chandigarh, 160014, India

ARTICLE INFO

Keywords:
Analytical chemistry
Natural product chemistry
Pharmaceutical chemistry
Solid state NMR
DSC
FTIR
Antihaemolytic
Pharmacokinetics
Daidzein
Antioxidant
Cocrystals
Anti-inflammatory
PXRD

ABSTRACT

The present study involves the contribution of cocrystallization towards the modification of the biopharmaceutical parameters of poorly watersoluble plant-originated isoflavone, daidzein (DAID). The cocrystals were prepared with GRAS status coformers i.e., isonicotinamide, theobromine and cytosine using mechanochemical grinding and characterized by various analytical techniques (DSC, FT-IR, PXRD and solid-state NMR). Crystal structures were obtained from PXRD data using BIOVIA Materials Studio software and compared in terms of supramolecular motifs. An additional qualitative and quantitative insight into interactions between both components of the cocrystal illustrated the presence of OH···N and OH···O=C heterosynthons and revealed a stabilizing role of hydrogen bonding. The cocrystals were further evaluated for their solubility, intrinsic dissolution and in vivo profile. Solubility and dissolution studies of pure daidzein and its cocrystals, namely daidzein-isonicotinamide (DIS), daidzein-cytosine (DCYT) and daidzein-theobromine (DTB) exhibited an almost 2-fold improvement. Evaluation of maximum concentration (Cmax) of cocrystals reveals that the DIS cocrystal shows the highest Cmax of 1848.7 ng/ml followed by DCYT cocrystal (1614.9 ng/ml) and DTB cocrystal (1326.0 ng/ml) in comparison to DAID which has a Cmax 870.5 ng/ml. Each of these cocrystals showed significant enhancement in *in vivo* and *in vitro* activities in comparison to daidzein. Thus, this report suggests cocrystallization as a viable approach to resolve the solubility and bioavailability issues that circumvent the use of a therapeutically potential isoflavone, daidzein.

1. Introduction

The recent formulations (of the newly discovered compounds) has resulted in the development of a range of supramolecular systems including solid dispersions, co-crystal as well as hybrid liquisolidsystems (Chen et al., 2012; Brus et al., 2017; Peer et al., 2007; Policianova et al., 2014). In this context crystal engineering has brought incommensurable advances in the field of solid–state chemistry to generate supermolecules with target structures and specific physiochemical parameters. Cocrystals are designated as one of the resultant products of crystal engineering strategy which usesnoncovalent intermolecular attractive forces with an intention to bring two or more different molecules into a unique crystal lattice. A key factor in designing of cocrystals relies on which of the two feasible intermolecular bonds i.e. heteromeric (cocrystal) or homomeric (single molecule) is witnessed. Molecules containing complementary functional groups are considered to be the potential source of supramolecular synthons for cocrystal generation (Oaki, 2017; Lusi, 2018). The technique of cocrystallization is a lucrative option which not only caters a drug candidate with desired physicochemical properties (Thakuria, 2018; Ueda, 2017) but also offers the right of intellectual property (IP) protection (Aakery and Salmon, 2005). Moreover, with high atom efficiency and no waste products make cocrystallization an important part of the green chemistry initiative(Cannon and Warner, 2002).

The present work reporting the cocrystals of DAID is in continuation of our ongoing project on the modification of biopharmaceutical parameters of flavonoidal molecules (Chadha et al., 2017a,b) through crystal engineering. Isoflavone DAID is mainly present in leguminous plants, especially in soybeans, soy foods, Pueraria lobate Ohwi (Leguminosae) (Coward et al., 1993; Adlercreutz, 1995) and holds promise in the effects of hypertension (Rivas et al., 2002), coronary heart disease (Tikkanen and Adlercreutz, 2000), cerebral thrombosis, and menopause syndrome (Möller et al., 2010).

Research has revealed that DAID exhibits as a potential isoflavone multiple pharmacological effects (Kurzer and Xu, 1997; Bingham et al., 1998; Setchell and Cassidy, 1999), such as antioxidant, anti-haemolytic and anti-inflammatory activities (Dwiecki et al., 2009; Liu et al., 2009;

* Corresponding author.
E-mail address: renukchadha@rediffmail.com (R. Chadha).

https://doi.org/10.1016/j.heliyon.2019.e02669
Received 20 October 2018; Received in revised form 19 June 2019; Accepted 14 October 2019

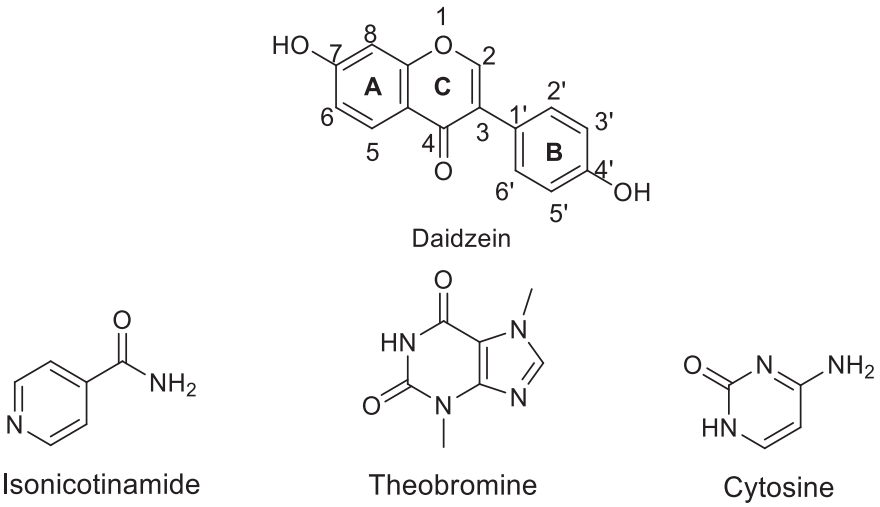

Scheme 1. Structures of daidzein and coformers.

Naim et al., 1976). Studies have shown that this phytoestrogen is also responsible for suppressing the growth of cancer cells by stimulating a cell death pathway which in turn accelerates the formation of bone cells and avert the onset of diabetes (Wang et al., 2002; Lo et al., 2007; Choi et al., 2008; Jin et al., 2009).These activities, along with low toxicity, make it important candidate for experimental lead compound for drug design. However, the pharmacological benefit rate of DAID is lower and the dose is more due to its poor solubility (Kulling et al., 2001). Animal experiments have demonstrated that after oral administration to rats the absolute bioavailability of DAID suspension is only 6.1% (Qiu et al., 2005), which seems to be the major culprit and can be related to the DAID's unfavorable physicochemical properties that include low solubility, low partition coefficient of oil/water, and, may be strong metabolism that occurs in the intestine and liver (Kulling et al., 2001). Ample evidences are available in the literature showing improvement of bioavailability through cocrystallization technique. Literature survey has suggested that the clinical effectiveness of isoflavones is due to their ability to produce metabolites such as dihydrodaidzein (DHD), tetrahydrodaidzein (THD), equol and O-Desmethylangolensin (O-DMA) in the gut (Heinonen et al., 1999). In particular, equol, a intestinal bacterial metabolite of daidzein, has recently received considerable attention, because its biological activities differ from those of its precursor and has been found to be more bioavailable than the parent molecule, daidzein (Setchell et al., 2002). Henceforth, it suggests that the low solubility of daidzein overrules over first pass metabolism and so, the bioavailability is attributed to its poor solubility. Thus, its poor lipophilicity and hydrophilicity, brings a major challenge in pharmaceutical applications for this molecule. Attempts to improve the solubility and bioavailability were made by incorporating this phytonutrient in cyclodextrins and their derivates (Cannavà et al., 2010; Lee et al., 2007; Stancanelli et al., 2007; Xavier et al., 2010), cyclodextrin/hydrophilicpolymermixtures (Borghetti et al., 2011), phospholipids (Gao et al., 2008; Zhang et al., 2011), surfactants (Whaley et al., 2006), nanoparticles (Ma et al., 2012). Moreover, chitosan microspheres (Ge et al., 2007), poly (l-lactide) (Sojitra et al., 2010), hyperbranched polyester (Zou et al., 2005), and emulsions (Shen et al., 2010) were used as potential carriers. These approaches have their own limitations. However, uncertain kinetics and neurotoxicity in nanopaticles (De Jong and Borm, 2008), gastric toxicity and huge bulk of cyclodextrins (Del Valle, 2004), stability issue of proteins in chitosan microspheres limit the success of these strategies. The pharmaceutical cocrystals that are designed through crystal engineering principle are widely used in the pharmaceutical industries and academia to overcome the issues of low solubility and bioavailability of potential API's (Shete et al., 2015). There is no formation of adducts, intermediates or any waste products which makes cocrystallization a key method of green chemistry. The procedure for cocrystallization requires the addition of miniscle amount of solvents. Moreover, cocrystals are patentable and their expanding IP portfolios have made this technique popular in the growing field of pharmaceutical companies. Enhancement of bioavailability of nutraceuticals by cocrystallization is very well documented in literature. Baicalein (BE) and nicotinamide (NCT) cocrystal have shown a 2.5 fold enhanced oral bioavailability (Sowa et al., 2012). Besides this Epigallocatechin-3-gallate cocrystal with isonicotinamide (EGCg–INA) showed a modest improvement of 1.37- and 1.05-times bioavailability relative to EGCg (Smith et al., 2013).

In this manuscript an attempt has been made to prepare cocrystals of daidzein with isonicotinamide (ISO), theobromine (TB) and cytosine (CYT). DAID contains weakly acidic phenolic hydroxyl groups which are unlikely to form salt with bases at physiological pH, but they are presumed to form OH….C=O, OH…. NHetc hydrogen bond interactions with molecules having complementary functional groups leading to cocrystallization.

Coformers used were selected based on their generally referred as safe (GRAS) status, structural/functional properties and high throughput the Cambridge Structural database (CSD) results. A paradigm based on molecular design in which cocrystal formers can be exploited for their ability to form supramolecular interaction with potential DAID molecule has been exercised. CSD statistics indicate that supramolecular heterosynthons -OH———COOH and –OH———N are strongly favored over corresponding supramolecular homosynthons. The coformers apart from having high solubility also exhibit various therapeutic uses. Isonicotinamide being a isomeric analogue of nicotinamide and a metabolite of isonicotinicthioamide and strongly induce apoptosis in leukemia cells and theobromine is widely used as a vasodilator,a diuretic and heart stimulant (Adamafio, 2013). Whereas, cytosine is one of pyrimidine, nucleotides present in DNA and RNA (Pedersen et al., 2014). Scheme 1 illustrates structures of DAID and coformers used in this report. Crystallization experiments resulted in three new isoflavone cocrystals, namely DIS (1:1), DTB (1:1) and DCYT (1:1).

2. Experimental

2.1. Materials

DAID (≥97%, Alfa Aesar, England), ISO (≥99%, Sigma Aldrich, USA), TB (≥98%, HI-MEDIA, Mumbai, India), CYT (≥98%, HI-MEDIA, Mumbai, India) and ethanol (≥99%, E. Merk Ltd, New Delhi, India) were procured and used as per requirement.

2.2. Design of cocrystals

DAID is a well-known isoflavone and to design its new crystalline forms it is necessary to know about the statistics of existing synthons of hydroxyl groups and carbonyl group with other functional groups present in the CSD. According to synthon approacha specific functional group present in the drug molecule andcoformer plays a vital role in the development of crystal forms (Yadav et al., 2009; Shan and Zaworotko, 2008). Preliminary search for propensity of functional group that may generate supramolecular synthon was conducted using ConQuest software (version 1.7) searching existing crystal structures (considered only organic compounds) in Cambridge Structural Database (CSD, version 5.36, Nov. 2014).

2.3. Synthesis

Three co-crystals of daidzein with isonicotinamide (DIS), cytosine (DCYT)and theobromine (DBT) were prepared via solvent assisted grinding. The cocrystals were prepared by combining 1:1 stoichiometric ratio of DAID (254 mg) with ISO (122.12 mg), TB (180.16 mg) and CYT (111.10 mg) in a pestle mortar. The mixture was ground with a pestle for 1 h in case of DIS and for 2 h for DTB and DCYT. The process was facilitated with drop-wise addition of ethanol (10ml). This process was repeated several times until a dry solid mixture for all the cocrystals i.e., DIS, DTB and DCYT was obtained. The bulk was then kept in a desiccator under controlled conditions for further analysis.

2.4. Identification and characterization

2.4.1. Differential scanning calorimetry (DSC)

DSC of all the samples was carried out using DSC Q20 (TA Instruments, USA). Samples (3–5 mg) were placed in sealed aluminium pans and were scanned at rampling rate of 10 °C min^{-1} under a dry nitrogen atmosphere (flow rate 50 mL min^{-1}). The data was collected by TA Q series Advantage software (Universal analysis 2000). The temperature range of DSC was from 0 °C to 350 °C.

2.4.2. Fourier transform-infra red spectroscopy (FTIR)

A Spectrum RX I FT-IR spectrometer (Perkin-Elmer, UK) was utilized in the KBr diffuse-reflectance mode (sample concentration 2 mg in 20 mg of KBr) over the range of 4000–400 cm^{-1}. Data was analyzed by using spectrum software.

2.4.3. Powder X- ray diffraction (PXRD)

PXRD patterns were analysed using an X'Pert PRO diffractometer system (Panalytical, Netherlands) with a Cu Kα radiation (1.54060 Å). The tube voltage and current were set at 45 kV and 40 mA respectively and the divergence slit and antiscattering slit were set at 0.48° during illumination on the 10 mm sample size, analysed from 5° and 50° in 2θ with a step size of 0.017°. The PXRD patterns obtained experimental were refined using X'Pert High Score software.

2.4.4. Solid state NMR (SSNMR)

The solid state 13C NMR spectra were acquired using a Joel Resonance JNM-ECX400II Instrument from IISC, Bangalore, India. The temperature at which data was obtained was 273 K having 1024 complex data points, acquisition time 29.1 s, for polarization relaxation delay time of 5s and a contact time of 2 ms.

2.4.5. Crystal structure determination

Powder X-Ray diffraction patterns were subjected to Materials Studio® software by BIOVIA system to determine the structures of the bioflavovoidal molecules as well as their respective cocrystals. The preliminary step which is involved during the crystal structure determination is the preprocessing and the preparation of the PXRD data for further indexing step. The preprocessing step is done by subtracting background, smoothening of the peaks and after that the stripping was carried out. The overall structure determination was carried out in the following four steps;

- **Indexing**: Indexing was performed using X-cell routine (Neumann, 2003) soas to obtain appropriate crystal lattice from the peak positions (5°–40° 2θ) of the experimental powder diffraction pattern. Further, the unit cell with maximum Figure of merits was selected and suitable cell was produced.
- **Pawley fitting**: The optimization of the unit cell was done by pawley refinement. Additionally, the search for space groups was carried out to produce an appropriate cell.
- **Structure solution**: The structures of bioflavonoidal molecule (DAID) and the respective coformers were sketched and geometrically optimized in DMOL3 module. These optimized structures were then imported into unit cell created by powder indexing and the atomic arrangement in the asymmetric unit was determined with full-profile comparison method in Powder Solve module with 10 simulated annealing cycles (Engel et al., 1999) and 21100000 iterations in each cycle.
- **Rietveld refinement**: The structure solution was finally refined using the Rietveld Refinement module (Rietveld, 1969). The final weighted Rietveld parameter value (Rwp value) defined as the similarity between the experimental and calculated diffraction patterns was obtained after rietveld refinement. Forcite Geometrical optimization was done on the structure solution generated and structure was exported in cif format.

2.5. Apparent solubility studies

Apparent solubility study was conducted by shaking an excess amount samples (approx. 50 mg) in 10 ml of phosphate buffer of pH 6.8 in a water bath shaker (MSW-275, Macroscientific Works, Delhi) at 37 °C for 24 h at 200 rpm. The resulting samples were filtered through a 0.45 μ membrane filter and quantitative analysis of DAID was done by HPLC. The samples were withdrawn at various time intervals (4 h and after 24 h) to make sure that the solution was in equilibrium. The residual material was then subjected to FTIR.

2.6. Intrinsic dissolution studies

Intrinsic dissolution of DAID and cocrystals was determined in phosphate buffer pH 6.8. Pellets of pure drug and cocrystals were added to the flask and the resulting slurry was shaken at 150 rpm at 37 °C in a constant temperature bath. An aliquot of slurry was withdrawn at multiple time points (15, 30, 45, 60, 90, 120, 180, 200, 240 and 300 min) and filtered through 0.45μm membrane filter which was further analyzed by HPLC.

2.7. High performance liquid chromatography

The concentration of DAID in the solubility and dissolution experiments was determined by a Waters Alliance HPLC system which includes a Waters 2695 separation module, a Waters 2996 Photodiode Array Detector, and a 4.6 mm × 150 mm SunFire C18, 5 μm column (Waters Corporation, Milford, MA). Stock solutions of DAID and cocrystals were prepared using phosphate buffer pH6.8 to obtain various concentrations of calibration standards (10, 20, 30, 40, 50, 60, 70, 80, 90, 100 μg/ml). Separations were conducted using the mobile phase of a mixture of methanol and 0.1% ortho phosphoric acid (62:38) pumped at a flow rate of 1.0 mL/min through the column at a temperature of 35 °C. The detector wavelength was set at 355 nm. Data acquisition and analysis were carried out using software Empower 2.0. The retention time of DAID is 4.43 min as evaluated by HPLC analysis, however concentration of DAID in respective cocrystal was analyzed.

2.8. Biological Studies(In vitro and In vivo studies)

For the *in vivo* pharmacokinetic and pharmacodynamic study, 4–5 weeks old male wistar rats (150–250 g) were procured and kept in Central Animal House for adaptation of environment. The animals were provided with standard pellet diet and water *ad libitum*. Experiments were performed as per guidelines of committee for the control and supervision on experiments on animals (CPC-SEA). The experimental protocol was approved by Institutional Animal Ethics Committee (I.A. E. C.) under approval no- PU/IAEC/S/15/04.

2.8.1. Antioxidant activity

The scavenging activity for DPPH (2, 2' diphenyl-1-picrylhydrazyl) free radicals of daidzein and its cocrystals was determined according to the procedure illustrated by Blios (1958) with suitable modifications (Mensor et al., 2001).The stock solution was prepared by dissolving 3.94mg (0.1 mM) DPPHwith 100 ml in 50:50 methanol and water. The working solution was obtained by mixing 1 ml stock solution with 1ml of cocrystal of various concentrations prepared were (10, 20, 40, 60, 80, 100 μg/ml) to obtain an absorbance at 517 nm using the spectrophotometer. Pure drug molecule and cocrystals could react with the DPPH solution for 45 min in the dark. Ascorbic acid was used as standard control. Then the absorbance (UV–Visible EZ201, Perkin Elmer, USA) was taken at 517 nm and converted into the percentage antioxidant activity using the following equation described

$$\%\text{Radical scavenging activity} = \frac{(\text{Absorbance of control} - \text{Absorbance of sample})}{(\text{Absorbance of control})} \times 100$$

2.8.2. Antihaemolytic activity

The anti-hemolytic activity of daidzein and its cocrystals was done on rat red blood cells (RBC) (Chaudhuri et al., 2007). RBC's were isolated from rats and collected in centrifuge tubes containing equal volume of alsever solution, then this solution was centrifuged at 3000 rpm for 10 min at 4 °C. Packed blood cells were washed with isotonic buffer solution (0.9% saline pH 7), this step was repeated thrice. Final cell volume (10% v/v) was suspended in isotonic buffer solution (pH 7). 500 μL of the final packed cells was added to 4.5 mL of hypotonic phosphate buffer saline solutions containing various concentrations of DAID and its cocrystals (50, 100, 150 μg/mL in hypotonic PBS pH 7) incubated for 10 min at room temperature and then and centrifuged for 15 min at 3000 rpm at 4 °C. The extent of haemolysis by daidzein and its cocrystals was evaluated by obtaining absorbance of the resulting supernatant at 540 nm by UV-Visible spectrophotometer (Perkin Elmer).

2.8.3. Anti-inflammatory evaluation using rat paw edema model

Anti-inflammatory activity was evaluated by the carrageenan-induced rat paw edema test (Guardia et al., 2001). Animals were procured from central animal facility: Panjab University and the protocols were duly approved by the Panjab University Animal Ethical Committee vide reference number PU/IAEC/S/14/126. All the animal studies were performed in accordance with guidelines of the Committee for Control and Supervision of Experiments on Animals (CPCSEA). India Wistar rats (180–200g) were procured, maintained in central animal house and provided with standard pellet diet and water *ad libtium*. Overnight fasted rats were divided into seven groups (n = 6) including

Group I: Served as control (Received vehicle).
Group II: Rats were given 0.1 ml of 1% carrageenan.
Group III: Rats were given diclofenac (10 mg/kg/i.p) 0.1ml of carrageenan.
Group IV: Rats were given DAID suspended in aqueous CMC (0.5%w/v) and 0.1ml of carrageenan.
Group V: Rats were given DIS suspended in aqueous CMC (0.5%w/v) and 0.1ml of carrageenan.
Group VI: Rats were given DTB suspended in aqueous CMC (0.5%w/v) and 0.1 ml of carrageenan.
Group VII: Rats were given DCYT suspended in aqueous CMC (0.5% w/v) and 0.1 ml of carrageenan.

Each animal was orally administered DAID and its cocrystals at a dose equivalent to 10 mg/kg 30 min before subcutaneous injection of carrageenan of 0.1 ml of 1% w/v in 0.9% saline. The placebo group received equivalent volumes of the vehicle (saline). Male wistar rats were injected with 0.1 ml of carrageenan and edema was measured using a digital plethysmometer Ugo Basile (model 7140, Italy) at 0, 1, 2, 3, 4and 5 h time interval. Edema volume was expressed for each animal as the percentage change in rat paw volume after carrageenan injection, compared with placebo group. The activity was compared with the effect of diclofenac administration (10 mg/kg).

2.9. Pharmacokinetic studies in rat plasma

Male Sprague–wistar rats were purchased and used for the kinetic studies. Animals were acclimated with regular feed and drinking water ad libitum. The dose administered was 10 mg/kg to the experimental rats. Approximately 0.2 ml of blood was harvested from the jugular vein cannula at various time points. Samples were stored in a freezer until the HPLC analysis.

Study protocol: Overnight fasted rats were divided into six groups (n = 6) including

Group I: Served as control (Received vehicle).
Group II**:** Rats were administered aqueous CMC (0.5%w/v)
Group III:Rats were given DAID suspended in aqueous CMC (0.5%w/v)
Group IV:Rats were received DIS suspended in aqueous CMC (0.5% w/v)
Group V:Rats were received DTB suspended in aqueous CMC (0.5% w/v)
Group VI: Rats were received DCYT suspended in aqueous CMC (0.5% w/v)

Sampling of plasma: Blood samples from the retro-orbital capillary plexus were withdrawn at specified intervals (15, 60, 120, 180, 240, 360, 420 min) from rats of all groups and centrifuged at 5000 rpm for 20 min to separate plasma from blood sample. The final volume was made to 1 mL with solvent and analyzed for DAID content by HPLC.

HPLC analysis of DAID in plasma: The calibration standards were made by spiking 100 μL of the fresh pure plasma from untreated rat with an appropriate amount of 1 mg/mL methanolic stock solution of DAID. The calibration standards made were of 5, 10, 15 and 20 μg/mL concentrations. Further, the samples were injected into the system at an injection volume of 20 μl, with mobile phase consisting of orthophosphoric acid: methanol (20:80) at a flow rate of 1.2 ml/min.

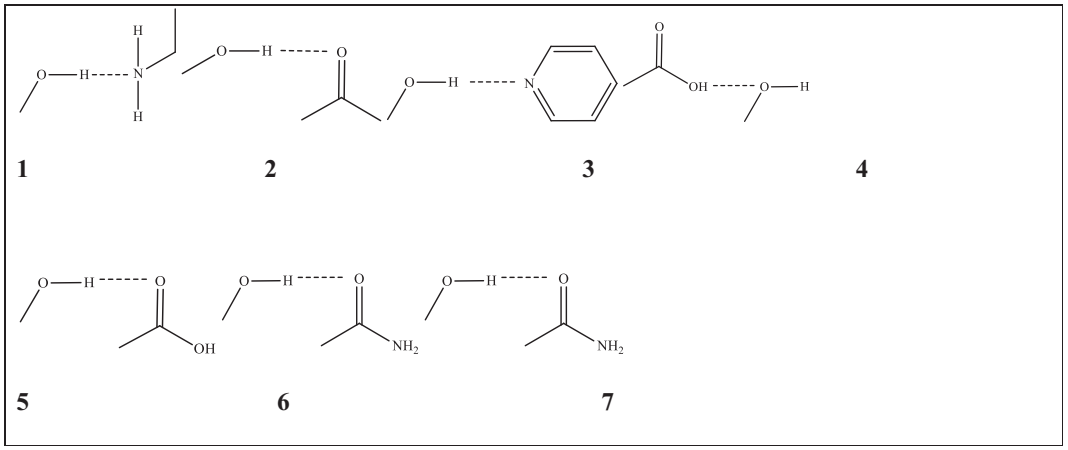

Fig. 1. Possible Supramolecular synthons.

Table 1
CSD statistics for potential functional groups.

S.No	Functional group present in drug	Potential functional groups	Supramolecular synthon	Hits
1	Hydroxyl group	Dimethylamine	1	1181
2	Hydroxyl group	Carbonyl group	2	4281
3	Hydroxyl group	Pyridine	3	3413
4	Hydroxyl group	Acetic acid	4	2044
5	Hydroxyl group	Acetic acid	5	5954
6	Hydroxyl group	Acetamide	6	609
7	Carbonyl group	Dimethylamine	7	1376

3. Results and discussion

Solvent-drop grinding was applied as a screening technique to identify new cocrystalline phases and their existence was confirmed by various analytical techniques. The identified cocrystals were afterwards evaluated for improvement in solubility, dissolution and pharmacokinetic profile. In addition to this antioxidant, anti-inflammatory and antiheamolytic activities were also performed.

3.1. Design of cocrystals and selection of coformers

Coformer selection is a vital step of the pharmaceutical cocrystal design technique since, the physiochemical properties of a coformer modulates the parameters of cocrystals. A hit and trial strategy were utilized traditionally in which the selected API would be tried with a series of coformers, which is expensive and time-consuming method. CSD is a worthy reference resource to study intermolecular interactions in the cocrystals and to find appropriate cocrystal pairs.

The CSD search was performed based on the functional moieties present in DAID which contains hydroxyl (OH) and carbonyl (C=O) groups. Search was conducted on each fragmented functional group and the hits were obtained from the database showing high propensity to generate multicomponent forms with certain functional groups. The possible supramolecular synthons with the hydroxyl group of the diadzein as per CSD search include 1, 2, 3, 4, 5 and 6 (Fig. 1) while the supramolecular synthon possible with carbonyl group of daidzein molecule is 7 (Fig. 1).

Based upon CSD search (Table 1), it was found that carboxylic acid group, aromatic nitrogen and carbonyl group are most susceptible to form hydrogen bond with hydroxyl group of DAID. Therefore, various coformers such as picolinic acid, nicotinic acid, histidine, cytosine, piracetam, theophylline, theobromine, isonicotinic acid, piperazine, picolinamide, 4-hydroxy benzamide, urea, acetamide, benzamide, pyridoxine, pyrogallol etc were tried. However, cocrystals could be formed with ISO, TB and CYT only.To explain why only three cocrystals were prepared a view on other influential factors responsible for cocrystal formation were studied. Various weaker interactions restrict the design of cocrystal and CSD utilization to discern and overcome any issues, governing the failure and success of cocrytal formation. Moreover, homologous compounds having the same functional groups, or the same possible synthons usually demonstrate different reactivity toward cocrystal formation, while some molecules can form cocrystals without any evident synthons linking them. Hence, it can be concluded that apart from reliable interaction there are other factors which govern the success of cocrystals such as shape and size mismatch and steric hinderance.

3.2. Characterization of Co-crystals

3.2.1. Differential scanning calorimetry

The cocrystals DIS, DCYT and DTB prepared by solvent assisted grinding technique were studied for their thermal behavior in relation to the individual components. Daidzein as well as the coformersISO, CYT and TB showed a single endotherm at 336 °C, 155.88 °C, 318.75 °C and 335.42 °C, in agreement with reported melting points. The DSC thermogram of the cocrystals showed a single endothermic transition attributed to the melting transition at 179.63 °C (DIS), 291.65 °C (DTB) and 276.88 °C (DCYT) (Fig. 2i, ii and iii). This distinct thermal behavior with different melting transition of cocrystals as compared to individual components signifies the formation of a new solid phase. The purity of the co-crystalline nature of the prepared material was assessed via DSC scans. The shape and position of the melting endothermic peaks represents the nature of the formed product. The narrow and sharp endotherm points towards a high degree of purity and crystallanity of the prepared noncovalent derivatives (Chadha et al., 2017a). Moreover, absence of melting endothermic peaks of coformer as well as drug molecule negates the presence of starting material indicating the purity of the cocrystalline phase.

A single endothermic event for the cocrystals indicates the absence of any unbound or absorbed solvent and exhibits the stability of the phase until the melting point.

Moreover, the sharp melting endotherm also negated the formation of co-amorphous phase. Additionally, the formation of cocrystals was further confirmed by FTIR, PXRD and solid-state NMR data.

3.2.2. Powder X-ray diffraction analysis

The PXRD pattern of DIS, DTB and DCYT displayed unique crystalline peaks when compared to DAID and their respective coformers demonstrating the formation of new solid forms. These unique patterns corresponding to each of the new solid phases are depicted in Fig. 3.

DIS shows characteristic new peak at (9.53°,12.24°,14.19° and

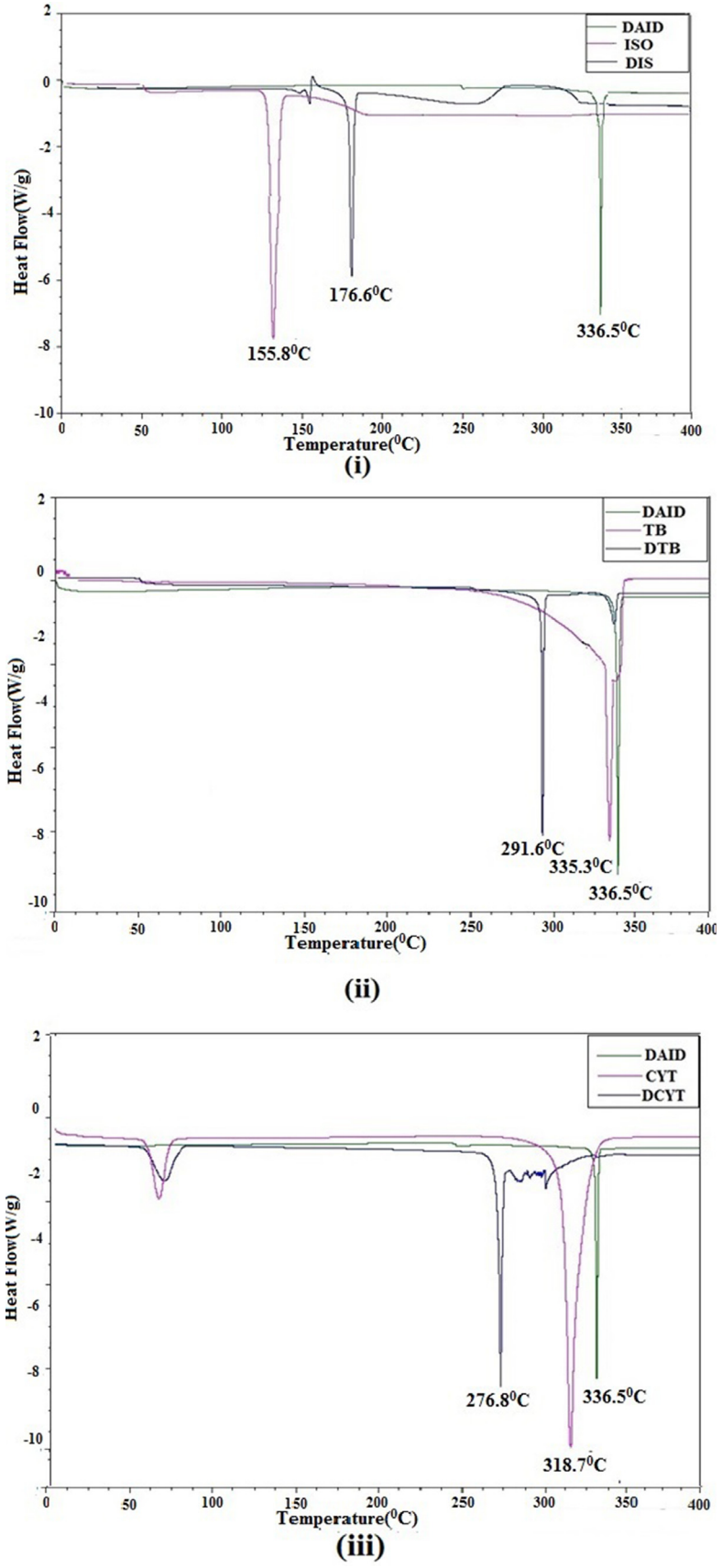

Fig. 2. Differential scanning thermogram of (i) DIS (ii) DTB (iii) DCYT

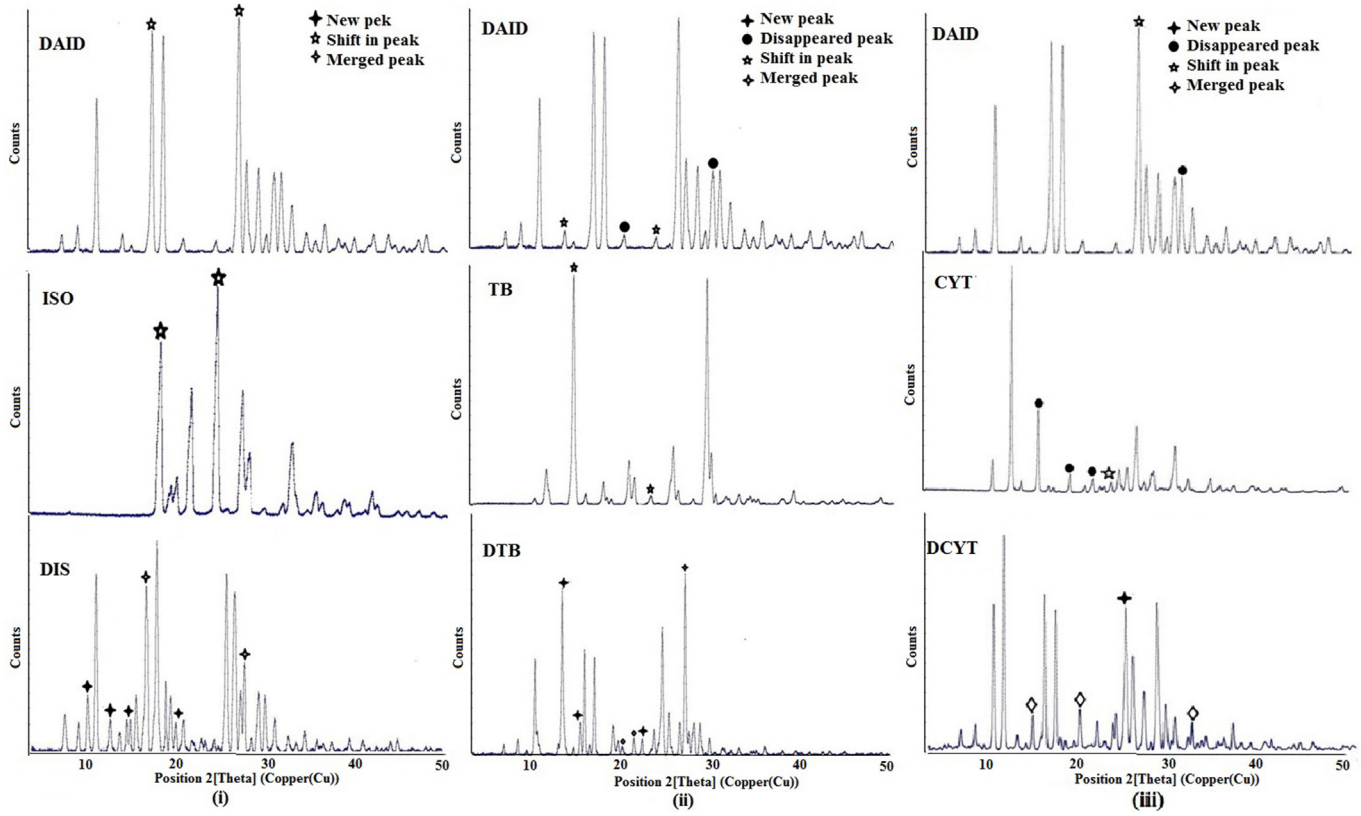

Fig. 3. PXRD pattern of DAID (i) DIS (ii) DTB and (iii) DCYT.

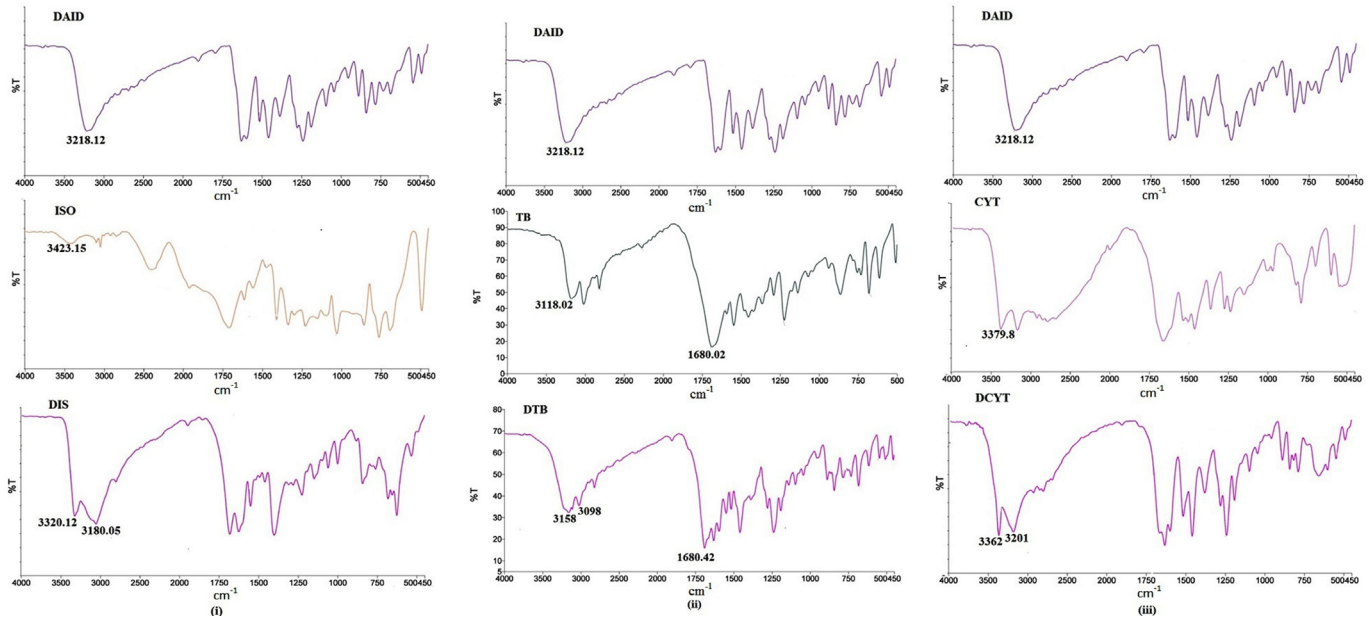

Fig. 4. FT- IR spectra of Daidzein (i) DIS (ii) DTB and (iii) DCYT.

19.77°) which are absent in the reflection patterns of DAID and ISO. Whereas, peaks (13.93°, 19.04° in DAID) has shifted to 13.74°, 19.20° in DIS. Concurrently the peaks at 15.95°, 24.62° in DAID and 16.82°, 24.10° have merged in DIS at 16.07° and 24.42 (2ɵ).

Similarly, DTB showed new peaks at 2θ values of 15.5° and 16.6°, 20.2°, 21.4°. In addition, peak at positions 19.0 and 28.08 which were present in DAID, are now absent in the pattern of DTB. Certain distinctive peaks of DAID at 13.0°, 23.3° and TB at 13.7°, 22.3° have merged to 13.4° and 22.4° in DTB. While peak at 9.7° and 12.4° in TB have shifted to 9.4° and 12.9° in DTB.

Similarly, in DCYT, new peaks at 14.82°, 18.76° and 31.63° which are absent in the reflection pattern of string molecules. Concurrently, the peaks at 23.76°, 24.62° in DAID and 23.63°,24.36° in CYT have merged at 23.55°,24.57° in DCYT cocrystal. Also, peaks at 16.50° and 19.91° in CYT and 28.17° in DAID no longer exist in the new solid phase.

The presence of distinguishable reflections in PXRD in collaboration

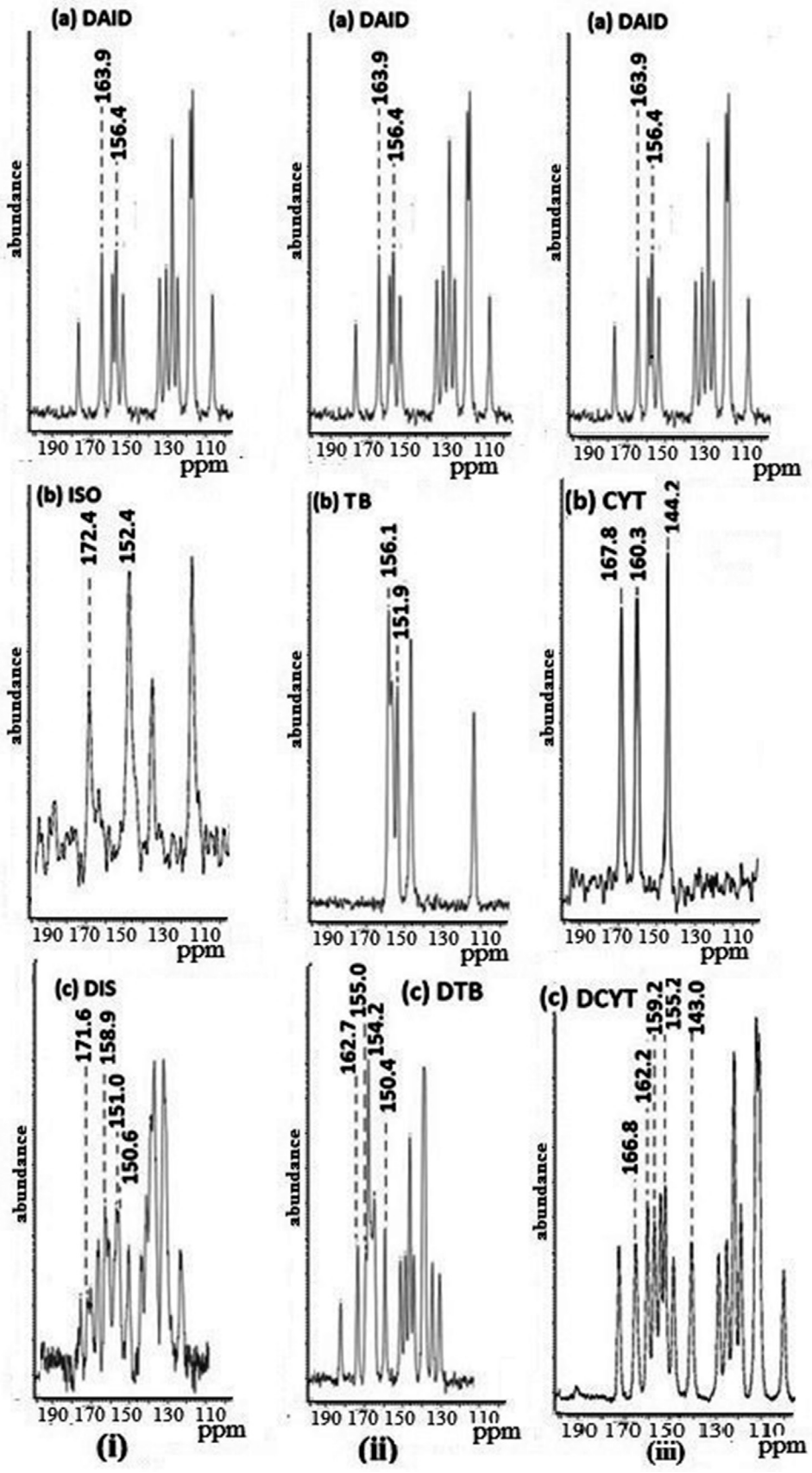

Fig. 5. Solid state NMR spectra of DAID (i) DIS (ii) DTB and (iii) DCYT.

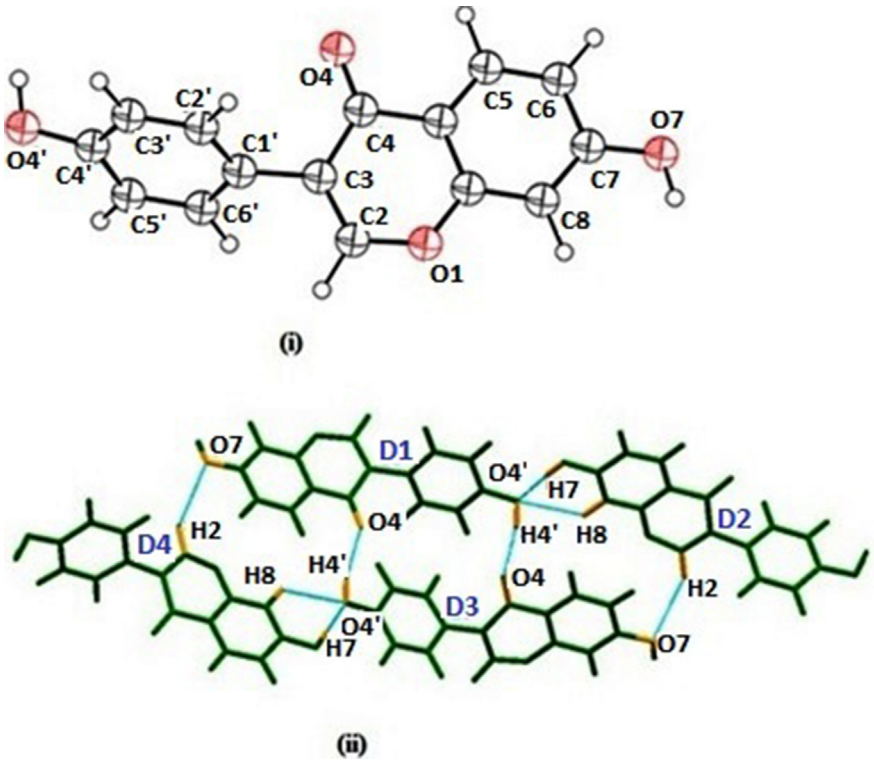

Fig. 6. (i) Asymmetric unit cell of daidzein (ii) Packing pattern of daidzein showing hydrogen.

with the distinct endothermic peaks in DSC, directs us one step closer to conclude the formation of a new cocrystalline phase in each case.

3.2.3. *Infrared spectroscopy*

FTIR is used for characterization of different cocrystals by recording shifts in the location and intensity of characteristic peaks. The FTIR spectrum of DAID showed several sharp characteristic peaks at 3218.12 cm^{-1} (corresponding to OH stretch), 2833.30 cm^{-1}(CH Stretch),1630.68 cm^{-1} (C=O Stretch) and 1598.50 cm^{-1}(C=C vibration). The changes in bands assigned to OH and C=O deformation in DAID were observed in the various cocrystals (Fig. 4).

After cocrystallization in case of DIS the vibrational frequency of OH stretch of DAID shifted from 3218.12 cm^{-1} to 3180.05 cm^{-1} while amide stretch of ISO shifted from 3423.15cm^{-1} to 3320.15 cm^{-1} conveying that certain kind of interaction is taking taking place between amide of ISO and hydroxyl group of DAID.

In case of DTB, shift of OH stretch from 3218.12 cm^{-1} to 3158 cm^{-1} in DAID, is accompanied by shift in NH stretch of amide of TB from 3118.02 cm^{-1} to 3098.0 cm^{-1} and stretching of carbonyl group shifts from 1688.20 cm^{-1} to 1680.42 cm^{-1}. This infers the interaction of hydroxyl group of DAID with amide group of TB.

In the IR spectrum of DCYT, significant shifts were seen in OH stretch from 3218.12 cm^{-1} to 3201 cm^{-1} in DAID, and N–H stretch of amine group in CYT shifted from 3379 cm^{-1} to 3362 cm^{-1} demonstrating interaction between these groups of DAID and CYT.

3.2.4. *Solid state NMR*

^{13}C SSNMR signals of DAID, TB, CYT, ISO, DTB, DCYT and DIS can be readily assigned according to chemical shifts. The cocrystal samples indicated slight changes in^{13}C chemical shifts with respect to the spectra of starting materials, which are attributed to the changed chemical environments linked with the formation of a new solid phase. Carbons which are chemically different in the cocrystal molecules are depicted by single resonance, and no peaks of phase impurities can be found in the ^{13}C spectrum. Therefore, it was deduced that the resulting phase is not a physical mixture of individual components, nor does it contain any impurities.

The ^{13}C SSNMR spectrum of the DIS co-crystal affirms for the advent of specific non-covalent interactions between DAID molecule and ISO molecule (Fig. 5i). This is confirmed by changes in the chemical shifts values of CH(C2), C–OH(C4′) of DAID and C–NH2(C4) and CH(C2) of ISO in cocrystal. Alteration in chemical shifts from 156.0 ppm at C4′ in DAID to 158.9 ppm and from 152.4 ppm at C2 of ISO to 150.6 ppm is observed in the DIS cocrystal spectra. Consequently, one of the hydroxyl group at C4′ is involved in a hydrogen bond, linking DAID molecule with aromatic nitrogen at N1 of ISO depicting acceptor-donor relationship. Similarly, there is a significant change in chemical shift of C2 of DAID from 152.4 ppm–151.0 ppm and C4 carbon in the vicinity of amide group of ISO from 172.4 ppm to 171.6 ppm. This indicates that the ketonic oxygen atom of DAID accepts hydrogen from amide group of ISO.

In the spectra of DTB, the signals from C4′ and C7 are found to be at 155.0 ppm and 162.7 ppm which has shifted from 156.4 ppm (C4′) and 163.9 ppm (C7) in DAID (Fig. 5ii). These shifts can be explained as a result of the involvement of both the hydroxyl groups of DAID in hydrogen bonding with neighboring DAID and TB molecules. Hydrogen of hydroxyl group at C4′ is involved in hydrogen bond formation with carbonyl oxygen attached to C2 of TB molecule with shift in chemical shift value from 151.3 ppm to 150.4 ppm forming O–H···O(C2) hydrogen bond. Whereas phenolic hydrogen at C7 is involved in the hydrogen bonding with another DAID molecule O–H···O(C4'). Moreover, the carbonyl oxygen at C6 of TB molecule shifts from 156.1 ppm to 155.0 ppm in cocrystal which is linked with the hydrogen of aromatic nitrogen of another TB molecule at N1 position.

The ^{13}C SSNMR spectrum of the DCYT co-crystal (Fig. 5iii) is evidence for the emergence of specific non-covalent interactions between CYT molecules and hydroxyl groups in DAID molecules. This is confirmed by changes in the chemical shifts of the carbon atom adjacent to OH in cocrystal molecules, as compared with the values of the chemical shifts of

Table 2
Crystallographic parameters.

Crystallography Parameters	DAID	DCYT	DIS	DTB
Chemical formula	C_{15} H_{10} O_4	C_{19} H_{15} N_3 O_5	C_{21} H_{16} N_2 O_5	C_{22} H_{18} N_4 O_6
Stoichiometry		1:1	1:1	1:1
Temperature	Room Temperature as specified 25 °C	Room Temperature as specified 25 °C	Room Temperature as specified 25 °C	Room Temperature as specified 25 °C
Crystal system	Orthorhombic	Orthorhombic	Triclinic	Triclinic
Cell volumes (A°3)	1130.228	3619.95	762	1351
Space group	Pnn_2	$PC_{21}B$	P_1	P_1
Cell lengths	a. 11.41440	a.15.5816	a.12.9126	a.13.50180
	b. 25.59260	b.11.2210	b.8.8758	b.11.36040
	c. 3.86900	c.20.7042	c.6.7529	c.10.05610
Cell angles (deg)	α = 90	α = 90	α = 80.985	α = 67.916
	β = 90	β = 90	β = 91.490	β = 107.974
	γ = 90	γ = 90	γ = 94.196	γ = 102.330
Z	4	4	2	2
2ɵ range	5° 45°	5° 45°	5° 45°	5° 45°
Rwp (%)	8.2	7.2	10.2	6.2

Table 3
Geometrical parameters of DAID cocrystals.

D–H····A	r (D–H) (A°)	r (H····A) (A°)	r (D···A) (A°)	r (D-H···A) (Deg)
DCYT				
O–H····N	0.957	2.382	3.302	143.10
DIS				
O–H····N	1.007	2.677	3.675	171.29
N–H····O	1.038	2.418	3.456	179.09
DTB				
O–H····O	0.960	1.679	2.634	172.87
N–H····O	1.008	2.009	2.986	162.58

atoms in the starting compounds. Similarly, the chemical shift of C7 of DAID changes from 163.9 ppm to 162.2 ppm along with shift in the peak position of C2 and C6 adjacent to aromatic nitrogen of CYT from 160.3 ppm (C2) to 159.2 ppm and 144.2 ppm (C6) to 143.0 ppm. This shows that the hydroxyl groups attached to C7 is involved in a hydrogen bond linking the DAID and CYT molecule, NH_2…. OH hydrogen bond formation. As a result, chemical shift decreased significantly from 156.0 ppm (C4′) of DAID to 155.2 ppm in cocrystal and C4 of CYT shows change from 167.8 ppm to 166.8 ppm in DCYT cocrystal. Indicating that the hydroxyl group at C4' of DAID is a proton acceptor accepting proton from amide group of CYT.

3.2.5. Structure determination

As already mentioned inthe manuscript, after various attempts to recrystalize the prepared cocrystals from various solvents we were not fortunate enough to grow a crystal with suitable size and of good diffraction quality for single crystal X-ray diffraction analysis Therefore, PXRD of the obtained cocrystals was used for the structure solution. It is worth mentioning that single crystal analysis and PXRD pattern contains the same intrinsic information. Whilst, the single crystal pattern is distributed in three-dimensional space, the PXRD data is compressed into one dimensional which generally leads to considerable overlapping of peaks. This issue can be resolved by different software having computational method (Harris and Tremayne, 1996; David and Shankland, 2008).

The simulated PXRD is well correlated with experimental PXRD, witnessed by low value of Rwp. The opinion of using PXRD for extracting the information at the molecular level is well corroborated by the growing number of structures solutions of solids determined annually using PXRD.

The crystal structure for DAID crystallized in Pnn_2 space group of the orthorhombic system. Packing pattern depicts four molecules of DAID involved in hydrogen bonding comprising of O7 (D1)····H2 (D4) whereas D3 molecule is attached to D4 molecule via H7 (D4)····O4′ (D3)···H8 (D4), and D3 is linked with D2 and D1 molecule by H4′ (D3)····O4 (D1), O4 (D3)····H4′ (D2) and O7 (D3)···H2 (D2) motifs (Fig. 6i and ii).

The cocrystals prepared form heteromic interactions by breaking the homomeric interactions amongst the DAID molecule.The cif files of DAID, DIS, DCYT and DTB have been submitted to CCDC (no. 1525244, 1525059, 1525061, 1525060). Crystallographic parameters and the geometrical parameters of DAID cocrystals are depicted in Tables 2 and 3.

The DIS (1:1) crystallizes in P_1 space group of the triclinic system, with two molecules of DAID and ISO which are inproximity with each other in an asymmetric cell (Fig. 7i). ISO molecule is linked with the DAID molecule through the involvement of N1·····H4′O4′ and N4H4···· O1 (Fig. 7ii) which give rise to in plane ring motif forming a two-dimensional hydrogen bonding. Packing pattern of DIS is illustrated in Fig. 7iii. The phenolic hydrogen on C4′ of DAID1 forms hydrogen bonding (O4′H4′···· N1) with aromatic nitrogen of ISO1. Additionally the amide group of one of the ISO molecule involved in hydrogen bonding (ISO1) donates its hydrogen (N4H4) to form hydrogen bonding (N4H4···· O1) with oxygen of the heterocyclic pyran ring (Fig. 7iv). Such an arrangement engages one donor hydroxyl substituents in DAID (C4′) and one acceptor (O1) whereas in ISO one donor N4H4 and one acceptor site N1. DAID and ISO are bound together between the planes of A/C rings of DAID and NH group of ISO by an angle of 50.63. Within those chains, the ISO and DAID molecules are not coplanar but form an angle of 67.53. The comparison of the experimental PXRD pattern and the stimulated PXRD pattern is depicted in Fig. 7v along with the Rwp values.

DTB crystallizes in P_1 space group of the triclinic system with one molecule each of DAID and TB in an asymmetry unit cell (Fig. 8i). Aggregates are held together by a cooperative arrangement connecting DAID and TB by hydrogen of phenolic group at C4′ position of DAID with oxygen of carbonyl carbon at position C2 of TB forming O4′H4′···· O2 motif (Fig. 8ii). The TB molecule exists as a dimer and interact via carboxamide group i.e., N1H1···O6. The oxygen of the carbonyl group at C2 position of TB is free to form hydrogen bonding with the hydrogen of phenolic group at C4′ of DAID i.e., O4′–H4′···O=C2. DAID molecules are also attached to each other by O7H7···O4′ (Fig. 8iii). Thus, a four-component assembly is formed by two molecules each of DAID and TBand the supramolecular interaction leads to the generation of two alternate layers (Fig. 8iv). On extending the hydrogen bonding pattern it has been observed that an alternate layer of DAID and TB are attached by hydrogen bonding. One hydrogen bond is formed between the nitrogen atom of the secondary amine of a TB molecule and the oxygen atom from a carbonyl group of another TB molecule (N–H···O), resulting in an R^2_2 (8)dimer (purple colored) in Fig. 8ii. An additional hydrogen bond between the oxygen of TB carbonyl group and the hydrogen of DAID hydroxyl group (O–H···O=C), (orange colored), leading to a twisted chain motif running along the b-axis. The comparison of the experimental PXRD pattern and the stimulated PXRD pattern is depicted in Fig. 8v

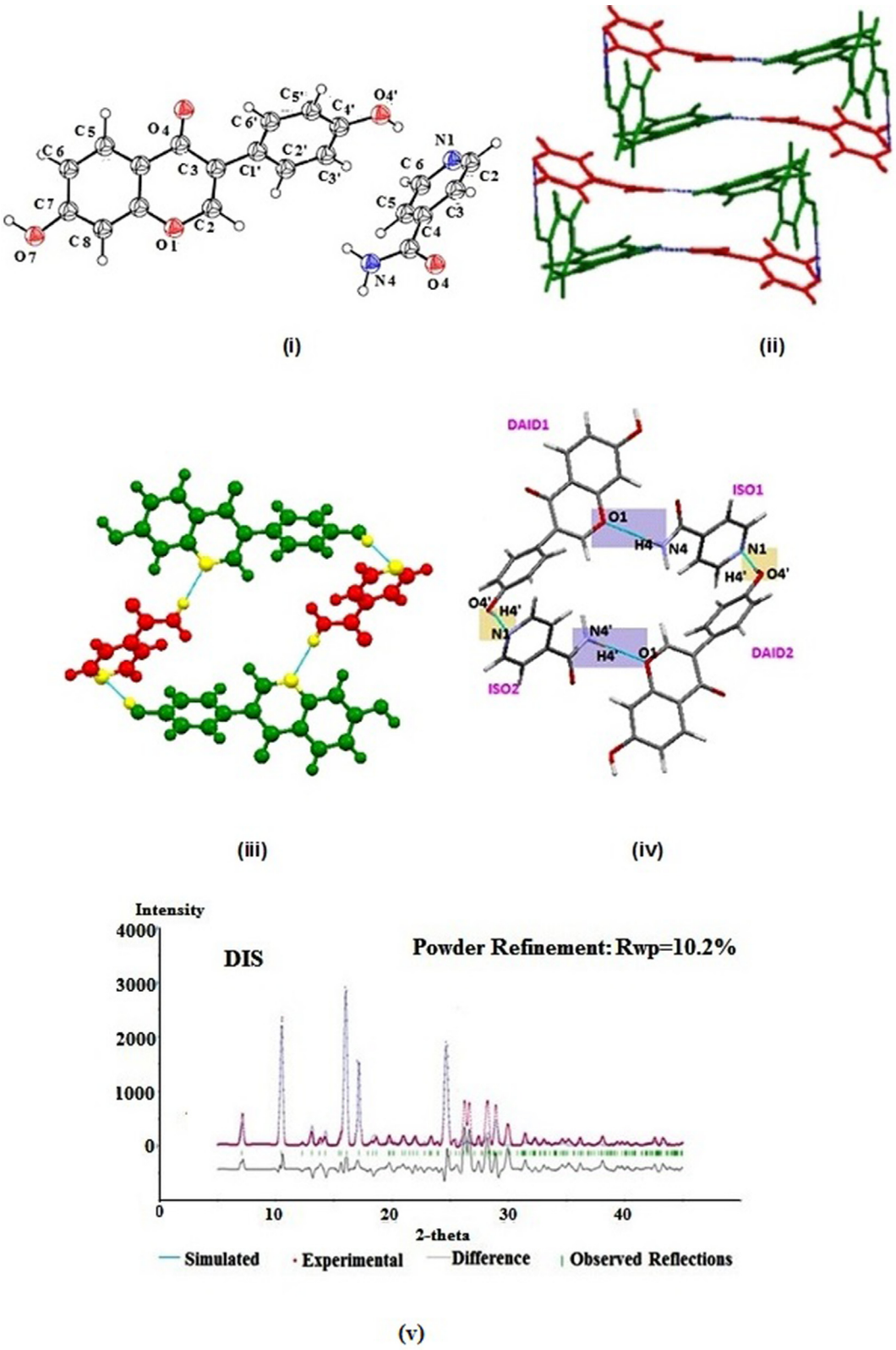

Fig. 7. (i) Asymmetric unit cell of DIS (ii) Packing arrangement of daidzein (green) and Isonicotinamide (red) in DIS (iii) Interaction of daidzein (green) and Isonicotinamide (red) by hydrogen bonding (blue) (iv) Packing pattern of DIS showing motifs. (v) The Rietveld plot of DIS cocrystal. Green coloured lines depict the observed reflections. Experimental data is shown by red dots and the stimulated data is shown by blue lines whereas, their difference is represented by black lines.

along with the Rwp values.

The DCYT cocrystal crystallizes in orthorhombic system with $PC_{21}B$ space group and its asymmetric unit is shown in Fig. 9i. In DCYT, the DAID molecule interacts with two molecules of CYT by means of OH–NH hydrogen bonds, namely, O4′H4′···· N4H4A and H7O7···N4H4B. The orientation of the molecules enables a close contact to be formed between amine group of CYT and hydroxyl group of DAID which serves to form a doubly bridging subunit (Fig. 9ii). The hydroxyl group attached at

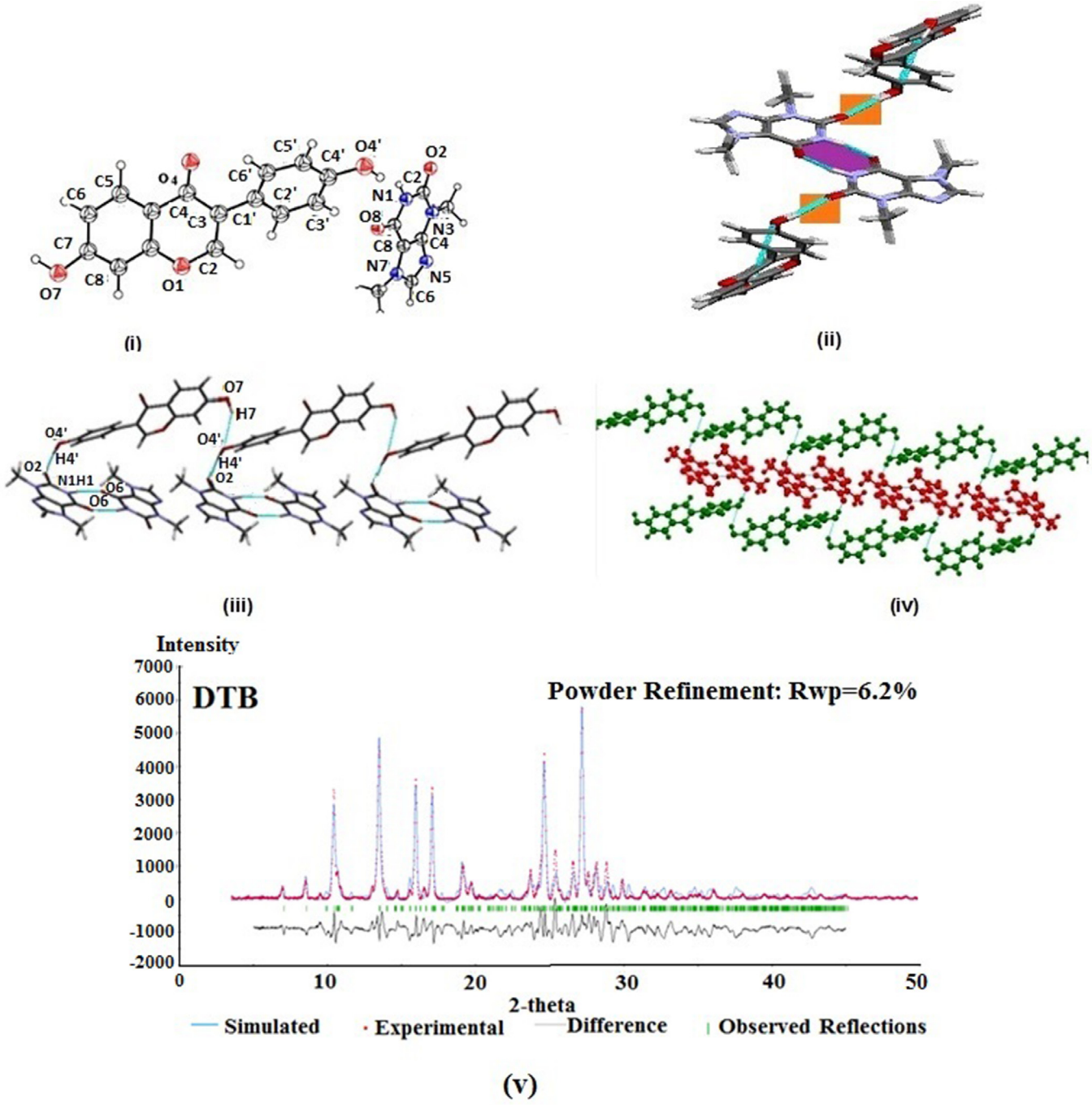

Fig. 8. (i) Asymmetric unit cell of DTB (ii) View of DAID:TB along b axis illustrating infinite chains of theobromine and stacking of daidzein molecules (iii) Packing pattern of DTB showing motifs (iv) Interaction of daidzein (green) and theobromine (red) by hydrogen bonding (blue) (v) The Rietveld plot of DTB cocrystal. Green coloured lines depict the observed reflections. Experimental data is shown by red dots and the stimulated data is shown by blue lines whereas, their difference is represented by black lines.

C4′ of DAID donates its hydrogen to nitrogen of CYT (N4) whereas the oxygen of the hydroxyl group attached at C4′ of DAID accepts the hydrogen from the amine of CYT (N4H4) (Fig. 9iii). The comparison of the experimental PXRD pattern and the stimulated PXRD pattern is depicted in Fig. 9iv along with the Rwp values.

3.3. Apparent solubility

Solubility of pure DAID and its cocrystals was assessed in phosphate buffer pH 6.8. Quantification of DAID was done by HPLC and the results are given in Table 5. The samples were analyzed after 4 h as well as after 24 h as discussed in the experimental section. The intrinsic dissolution studies results showed that maximum solubility levels for DIS and DCYT was achieved after 180 min whereas in case of DTB was observed after 200 min. Consequently, a decrease in the enhancement of the solubility of the cocrystals was seen after Smax. The solubility of daidzein cocrystals was found to be much less after 24 h indicating the breakdown of the cocrystals into the individual consituents. The improvement in solubility of cocrystalsupto 4 h period is enough for the drug molecule to elicit their pharmacokinetic and pharmacodynamic activity. This phenomenon is

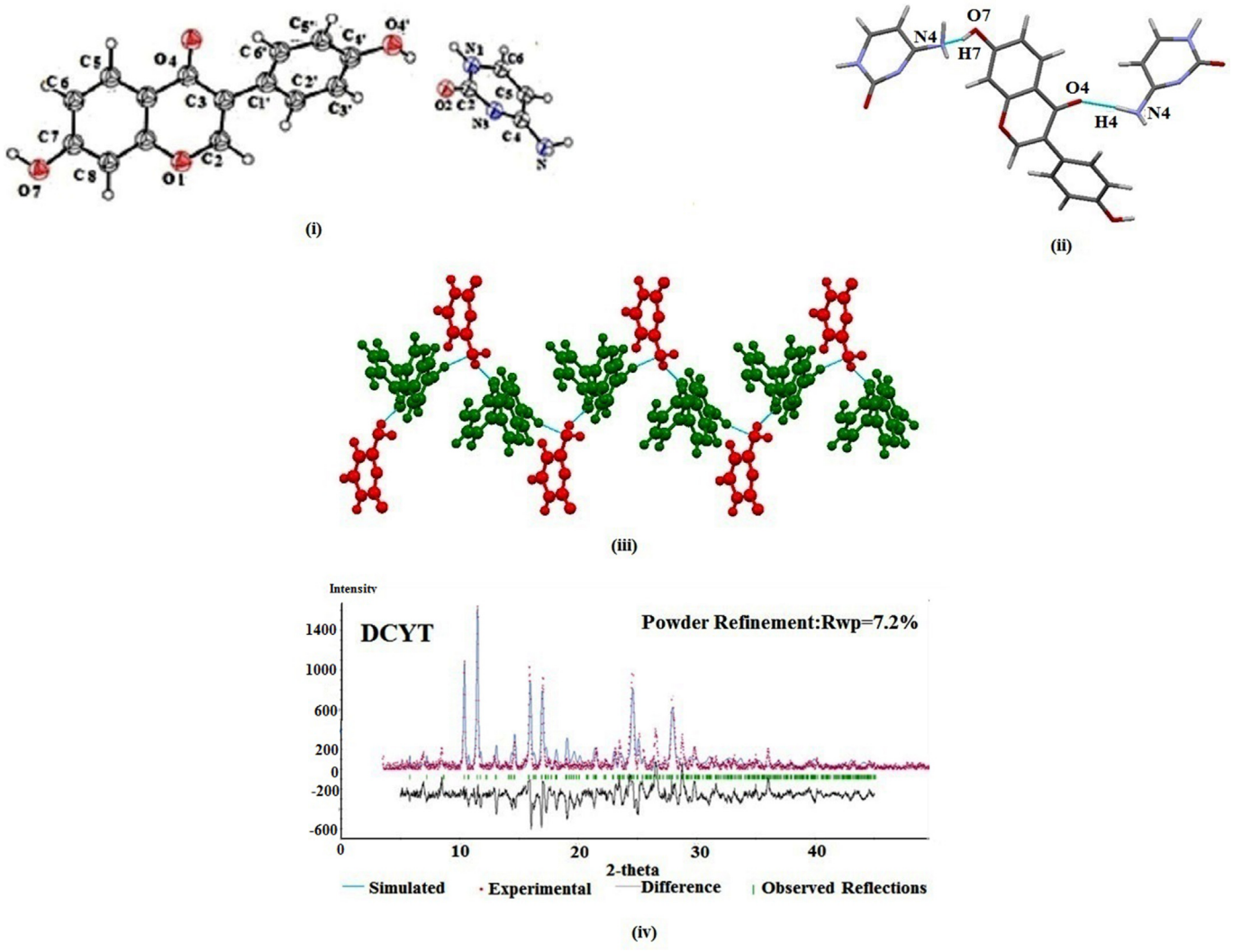

Fig. 9. (i) Asymmetric unit cell of DCYT (ii) Packing pattern of DCYT showing motifs (iii) Interaction of daidzein (green) and cytosine (red) by hydrogen bonding (blue). (iv) The Rietveld plot of DCYT cocrystal. Green coloured lines depict the observed reflections. Experimental data is shown by red dots and the stimulated data is shown by blue lines whereas, their difference is represented by black lines.

well known as spring and parachute effect which has been depicted by most of the pharmaceutical cocrystals (Lin et al., 2013; Sanphui et al., 2011; Cheney et al., 2011; Gangavaram et al., 2011; Alatas et al., 2015; Sarkar and Rohani, 2015).

As per this phenomenon after the breakdown of a cocrystal (DIS and DCYT after 180 min whereas in case of DTB after 200 min), the coformer which is more soluble constituent in a cocrystal is drawn out of the crystal lattice into the aqueous phase. Whereas, the hydrophobic component i.e., the nutraceutical component becomes supersaturated inthe biological medium. This high energy form of the nutraceutical component known as the "Spring" and immediately settlesdownto loosely aggregated clusters. However, this phase lasts for enough time period to facilitate adequate absorption to take place.

Comparison of solubility and IDR of cocrystals and with that of DAID reveals that the DIS (29.69 mcg/ml) cocrystal is almost 2.10 times more soluble than parent DAID (14.09 mcg/mg) followed by DCYT (26.97 mcg/ml) cocrystal which is 1.9 times more soluble. It is followed by DTBcocrystal which is 1.7 times more soluble throughout most of the experiment. Maximum solubility (S_{max}) is given in Table 4.

Solubility of coformers, its melting point and strength of hydrogen bond with drug contributes for the enhanced solubility and dissolution aspects of the cocrystals. Additionally, the highest solubility of DIS is ascribed to the fact that ISO has highest solubility and lowest melting point.

FTIR analysis was carried out on the residual material of the solubility studies after 4 and 24 h to examine any significant changes in the co-crystals. The FT-IR results showed that the cocrystals were intact up to 4hours.However, after 24 h of the study the FT-IR pattern is similar tothat of DAID. Therefore, it can be concluded that there has been a conversion of co-crystals to DAID after 24 h (Fig. 10).

3.4. Pharmacokinetic studies

To evaluate whether the bioavailability of flavonoids have been improved through crystal engineering, the pharmacokinetic experiment of DAID and cocrystals were carried out. The pharmacokinetic curves for cocrystals and pure drug are presented in Fig. 11. The cocrystals exhibited an improved pharmacokinetic profile compared with pure component. The pharmacokinetic parameters are shown in Table 5. Notably, DIS cocrystal has changed the overall shape of the pharmacokinetic curve with higher C-max, shorter T-max and AUC0−12 h in comparison to DAID and other cocrystals component. This increase in AUC in case of DIS is correlated with its faster dissolution rate and higher solubility. Based on this, a cocrystallization approach with GRAS status

Table 4
Maximum solubility and IDR.

	Solubility (μg ml $^{-1}$)	IDR (mcg min $^{-1}$ cm^{-2})
DAID	14.09 ± 0.03	29.52 ± 0.02
DIS	29.69 ± 0.05	45.9 ± 0.05
DCYT	26.97 ± 0.02	43.9 ± 0.03
DTB	24.84 ± 0.03	39.14 ± 0.03

coformers is proven to be a feasible technique to ameliorate the potential of DAID and progress the development of pharmaceutical cocrystals.

3.5. Accelerated stability study

The cocrystals of DAID were subjected to accelerated stability conditions at 40°C/75% RH for 3 months and characterized by DSC and PXRD. The results showed that all the cocrystals were stable and no significant changes were observed in DSC (Table 6) and PXRD pattern.

3.6. Biological studies

3.6.1. Antioxidant activity

The DPPH radical scavenging activity of analyzed cocrystals was compared to ascorbic acid, a known antioxidant agent. The antioxidant activity for DPPH assay of pure DAID and its cocrystals differ significantly due to the variability in solubility profiles. As shown in Fig. 12, percentage of DPPH radical scavenging activity was increased in a concentration-dependent manner in all three cocrystals. In comparison, the DIS cocrystal exhibited the strongest activity with (% inhibition 64.08 at 100 μg/ml), whereas the DCYT and DTB cocrystals showed comparable activity.

3.6.2. Antihemolytic activity

From the results obtained, RBC treated with the pure drug and its

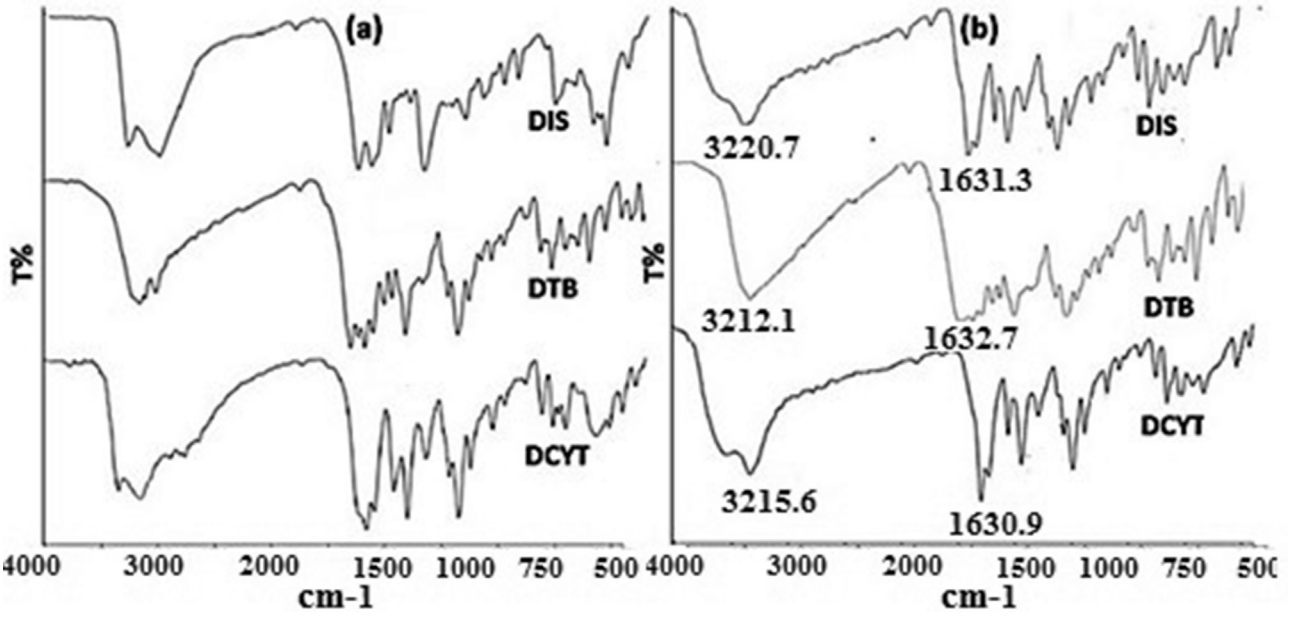

Fig. 10. FT-IR spectra of the residual material after (a) 4 h and (b) 24 h of the solubility study.

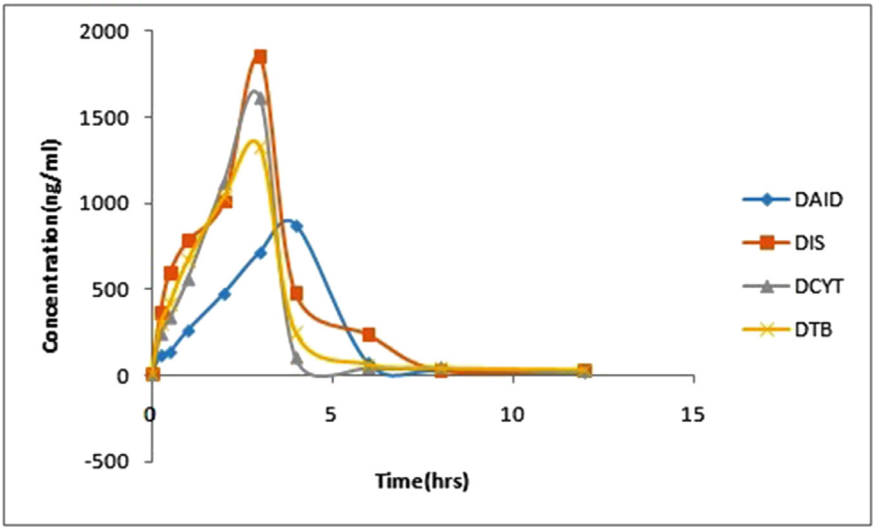

Fig. 11. Pharmacokinetic profile of daidzein and its respective cocrystals.

Table 5
Pharmacokinetic parameters.

S.NO	Cmax (ng/ml)	Tmax (hr)	MRT (hr)	$AUC_{0\text{-}2}$ (ng/ml)*hr	Relativebioavailability
DAID	870.5 ± 0.02	4	2.5	1282.29	
DIS	1848.7 ± 0.05	3	2.4	2702.40	2.10
DCYT	1614.9 ± 0.03	3	2.4	2451.08	1.91
DTB	1326.0 ± 0.02	3	2.9	2206.16	1.72

Table 6
Melting point of samples after 3 months.

Samples	Melting point	Melting point after 3 months
DIS	179.63 °C	180.63 °C
DCYT	276.88 °C	275.31 °C
DTB	291.65 °C	289.25 °C

respective cocrystals observed a marked reduction in haemolysis. Haemolysis of the RBC decreased with increase in the concentrations.

All cocrystals exhibited satisfactory inhibitory properties against hemolysis (Fig. 13). The DIS inhibited hemolysis with 69.76% as maximum anti-hemolytic activity at 150 μg/ml. The maximum anti-hemolytic activities of DCYT and DTB were 65.78% and 57.6412 respectively at a concentration of 150 μg/ml. Among these three cocrystal, the DIS represented the strongest efficiency followed by the DCYT and DTB, respectively.

3.6.3. *Anti-inflammatory activity*

The results of anti-inflammatory activity demonstrated that cocrystals of DAID were able to reduce rat paw induced by carrageenan (Fig. 14). These results are inagreement with the dissolution pharmacokinetic profiles which have shown the cocrystals to be more soluble as compared to DAID, and out of these, further; the form DIS is much more soluble than DCYT and DTB.

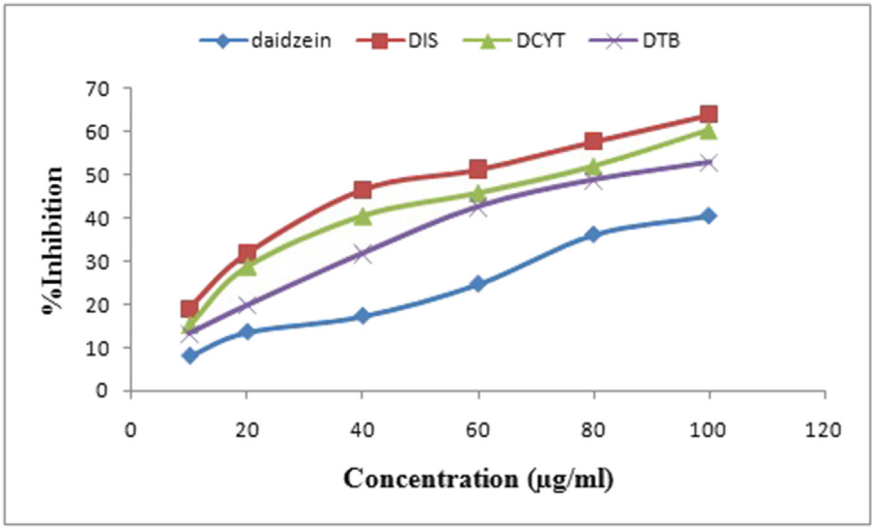

Fig. 12. Antioxidant activity of daidzein and its respective cocrystals.

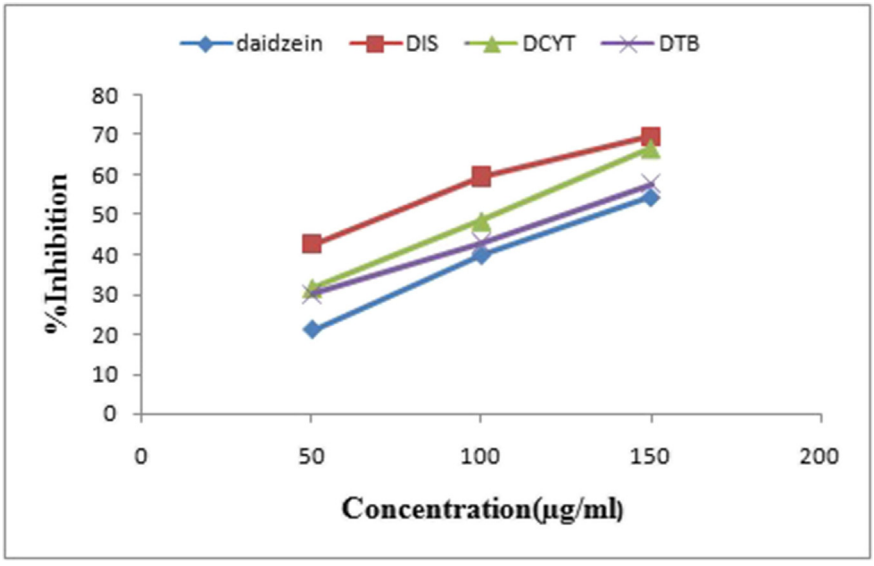

Fig. 13. Antihaemolytic activity of daidzein and its respective cocrystals.

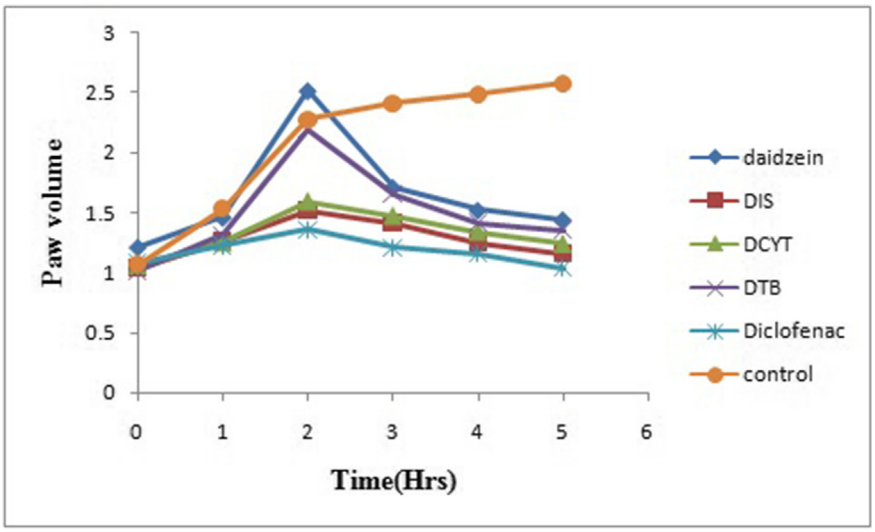

Fig. 14. Anti-inflammatory activity of daidzein and its respective cocrystals.

4. Conclusion

An endeavor has been made to provide an insight into crystal engineering of daidzein by preparing and characterizing its cocrystals in 1:1 ratio i.e., DIS, DCYT and DTB. A screening experiment using solvent assisted grinding was performed which had enabled the identification of the generated cocrystalline phase. The characterization of the obtained cocrystalline phases was carried out in terms of thermal and spectral properties. The crystal structures elucidation is correlated with the spectral data of the prepared cocrystals suggesting the intermolecular contacts established within the cocrystals. In all the three cases DAID was found to be engaged in hydrogen bond with the complementary functional groups of the CYT (C=O), TB (OH) and ISO (OH). The success of cocrystallization to enhance the physiochemical parameters and optimize the bioavailability of daidzein has been illustrated by the improvements in solubilitystudies. Moreover, the results of solubility studies are in agreement with the *in vitro* activities (antioxidant evaluation and antihemolytic studies) as well as the *in vivo* experiment (anti-inflammatory activity). It is noteworthy that the cocrystals present a considerably improved performance with a sharply increased Cmax and AUC with respect to pure components. However, in the present study pharmaceutical parameters including compactility, tabletability and compressibility have not been covered and will be taken up in our next publication. These results clearly demonstrate the improvement in solubility and bioavailability of daidzein through cocrystallization.

Declarations

Author contribution statement

Renu Chadha: Conceived and designed the experiments; Wrote the paper.

Yashika Bhalla: Performed the experiments, analyzed anad interpreted the results; Wrote the paper.

Kunal Chadha: Analyzed and interpreted the data; Wrote the paper.

Maninder Karan: Analyzed and interpreted the data; Contributed reagents, materials, analysis tools or data; Wrote the paper.

Funding statement

This work was supported by Department of Science and Technology (DST), New Delhi (File number: SR/SI/OC-90/2012) and University Grants Commission (UGC-RFMS), New Delhi (F.5-94/2007(BSR).

Competing interest statement

The authors declare no conflict of interest.

Additional information

Data associated with this study has been deposited at CCDC under the accession numbers 1525244, 1525059, 1525061, and 1525060.

References

Aakery, C.B., Salmon, D.J., 2005. Building co-crystals with molecular sense and supramolecular sensibility. CrystEngComm 72 (7), 439–448.

Adamafio, N., 2013. Theobromine toxicity and remediation of cocoa by-products: an overview. J. Biol. Sci. 13 (7), 570–576.

Adlercreutz, H., 1995. Phytoestrogens: epidemiology and a possible role in cancer protection. Environ. Health Perspect. 103 (Suppl 7), 103.

Alatas, F., Ratih, H., Soewandhi, S.N., 2015. Enhancement of solubility and dissolution rate of telmisartan by telmisartan-oxalic acid cocrystal formation. Int. J. Pharma. Sci. 7, 5–8.

Bingham, S., Atkinson, C., Liggins, J., Bluck, L., Coward, A., 1998. Phyto-oestrogens: where are we now? Br. J. Nutr. 79 (5), 393–406.

Blios, M.S., 1958. Antioxidant determination by the use of stable free radical. Nature 26, 1199.

Borghetti, G.S., Pinto, A.P., Lula, I.S., Sinisterra, R.D., Teixeira, H.F., Bassani, V.L., 2011. Daidzein/cyclodextrin/hydrophilic polymer ternary systems. Drug Dev. Ind. Pharm. 37 (8), 886–893.

Brus, J., Albrecht, W., Lehmann, F., Geier, J., Czernek, J., Urbanova, M., Kobera, L., Jegorov, A., 2017. Exploring the molecular-level architecture of the active compounds in liquisolid drug delivery systems based on mesoporous silica particles: old tricks for new challenges. Mol. Pharm. 14, 2070–2078.

Cannavà, C., Crupi, V., Ficarra, P., Guardo, M., Majolino, D., Mazzaglia, A., et al., 2010. Physico-chemical characterization of an amphiphilic cyclodextrin/genistein complex. J. Pharm. Biomed. Anal. 51 (5), 1064–1068.

Cannon, A.S., Warner, J.C., 2002. Noncovalent derivatization: green chemistry applications of crystal engineering. Cryst. Growth Des. 2 (4), 255–257.

Chadha, K., Karan, M., Bhalla, Y., Chadha, R., Khullar, S., Mandal, S., et al., 2017a. Cocrystals of hesperetin: structural, pharmacokinetic, and pharmacodynamic evaluation. Cryst. Growth Des. 17 (5), 2386–2405.

Chadha, R., Bhalla, Y., Nandan, A., Chadha, K., Karan, M., 2017b. Chrysincocrystals: characterization and evaluation. J. Pharm. Biomed. Anal. 134, 361–371.

Chaudhuri, S., Banerjee, A., Basu, K., Sengupta, B., Sengupta, P.K., 2007. Interaction of flavonoids with red blood cell membrane lipids and proteins: antioxidant and antihemolytic effects. Int. J. Biol. Macromol. 41 (1), 42–48.

Chen, B., Wang, Z.H., Quan, G.L., PengX, S., Pan, X., Wang, R.C., Xu, Y.H., Li, G., Wu, C.B., 2012. In vitro and in vivo evaluation of ordered mesoporous silica as a novel adsorbent in liquisolid formulation. Int. J. Nanomed. 7, 199–209.

Cheney, M.L., Weyna, D.R., Shan, N., Hanna, M., Wojtas, L., Zaworotko, M.J., 2011. Coformer Selection in Pharmaceutical Cocrystal Development:a Case Study of a Meloxicam Aspirin Cocrystal that Exhibits Enhanced Solubility and Pharmacokinetics, 100. Wiley Online Library, pp. 2172–2181.

Choi, M., Jung, U., Yeo, J., Kim, M., Lee, M., 2008. Genistein and daidzein prevent diabetes onset by elevating insulin level and altering hepatic gluconeogenic and

lipogenic enzyme activities in non-obese diabetic (NOD) mice. Diabetes/Metab. Res. Rev. 24 (1), 74–81.
Coward, L., Barnes, N.C., Setchell, K.D., Barnes, S., 1993. Genistein, daidzein, and their beta-glycoside conjugates: antitumor isoflavones in soybean foods from American and Asian diets. J. Agric. Food Chem. 41 (11), 1961–1967.
David, W., Shankland, K., 2008. Structure determination from powder diffraction data. Acta Crystallogr. Sect. A: Foundations of Crystallography 64 (1), 52–64.
De Jong, W.H., Borm, P.J., 2008. Drug delivery and nanoparticles: applications and hazards. Int. J. Nanomed. 3 (2), 133.
Del Valle, E.M., 2004. Cyclodextrins and their uses: a review. Process Biochem. 39 (9), 1033–1046.
Dwiecki, K., Neunert, G., Polewski, P., Polewski, K., 2009. Antioxidant activity of daidzein, a natural antioxidant, and its spectroscopic properties in organic solvents and phosphatidylcholine liposomes. J. Photochem. Photobiol. B Biol. 96 (3), 242–248.
Engel, G.E., Wilke, S., König, O., Harris, K.D.M., Leusen, F.J.J., 1999. PowderSolve - a complete package for crystal structure solution from powder diffraction patterns. J. Appl. Crystallogr. 32, 1169–1179.
Gangavaram, S., Suresh, K., Pal, S., Manjunatha, S.G., Nambiar, S., Nangia, A., 2011. Novel Furosemide Cocrystals and Selection of High Solubility, 101. Wiley Online Library, pp. 664–680.
Gao, Y., Gu, W., Chen, L., Xu, Z., Li, Y., 2008. The role of daidzein-loaded sterically stabilized solid lipid nanoparticles in therapy for cardio-cerebrovascular diseases. Biomaterials 29 (30), 4129–4136.
Ge, Y.B., Chen, D.W., Xie, L.P., Zhang, R.Q., 2007. Optimized preparation of daidzein-loaded chitosan microspheres and in vivo evaluation after intramuscular injection in rats. Int. J. Pharm. 338 (1), 142–151.
Guardia, T., Rotelli, A.E., Juarez, A.O., Pelzer, L.E., 2001. Anti-inflammatory properties of plant flavonoids.Effects of rutin, quercetin and hesperidin on adjuvant arthritis in rat. Il Farmaco 56 (9), 683–687.
Harris, K.D., Tremayne, M., 1996. Crystal structure determination from powder diffraction data. Chem. Mater. 8 (11), 2554–2570.
Heinonen, S., Wähälä, K., Adlercreutz, H., 1999. Identification of isoflavone metabolites dihydrodaidzein, dihydrogenistein, 6′-OH-O-dma, and cis-4-OH-equol in human urine by gas chromatography–mass spectroscopy using authentic reference compounds. Anal. Biochem. 274 (2), 211–219.
Jin, S., Zhang, Q., Kang, X., Wang, J., Zhao, W., 2009. Daidzein induces MCF-7 breast cancer cell apoptosis via the mitochondrial pathway. Ann. Oncol. 21 (2), 263–268.
Kulling, S.E., Honig, D.M., Metzler, M., 2001. Oxidative metabolism of the soy isoflavonesdaidzein and genistein in humans in vitro and in vivo. J. Agric. Food Chem. 49 (6), 3024–3033.
Kurzer, M.S., Xu, X., 1997. Dietary phytoestrogens. Annu. Rev. Nutr. 17 (1), 353–381.
Lee, S.-H., Kim, Y.H., Yu, H.-J., Cho, N.-S., Kim, T.-H., Kim, D.-C., et al., 2007. Enhanced bioavailability of soy isoflavones by complexation with β-cyclodextrin in rats. Biosci. Biotechnol. Biochem. 71 (12), 2927–2933.
Lin, Y., Yang, H., Yang, C., Wang, J., 2013. Preparation, characterization, and evaluation of dipfluzine–benzoic acid co-crystals with improved physicochemical properties. Pharm. Res. 1–13.
Liu, M.-H., Lin, Y.-S., Sheu, S.-Y., Sun, J.-S., 2009. Anti-inflammatory effects of daidzein on primary astroglial cell culture. Nutr. Neurosci. 12 (3), 123–134.
Lo, F., Mak, N., Leung, K., 2007. Studies on the anti-tumor activities of the soy isoflavonedaidzein on murine neuroblastoma cells. Biomed. Pharmacother. 61 (9), 591–595.
Lusi, M., 2018. Engineering crystal properties through solid solutions. Cryst. Growth Des. 18 (6), 3704–3712.
Ma, Y., Zhao, X., Li, J., Shen, Q., 2012. The comparison of different daidzein-PLGA nanoparticles in increasing its oral bioavailability. Int. J. Nanomed. 7, 559.
Mensor, L.L., Menezes, F.S., Leitão, G.G., Reis, A.S., Santos, TCd, Coube, C.S., et al., 2001. Screening of Brazilian plant extracts for antioxidant activity by the use of DPPH free radical method. Phytother Res. 15 (2), 127–130.
Möller, F.J., Diel, P., Zierau, O., Hertrampf, T., Maaß, J., Vollmer, G., 2010. Long-term dietary isoflavone exposure enhances estrogen sensitivity of rat uterine responsiveness mediated through estrogen receptor α. Toxicol. Lett. 196 (3), 142–153.
Naim, M., Gestetner, B., Bondi, A., Birk, Y., 1976. Antioxidative and antihemolytic activities of soybean isoflavones. J. Agric. Food Chem. 24 (6), 1174–1177.
Neumann, M.A., 2003. X-Cell: a novel indexing algorithm for routine tasks and difficult cases. J. Appl. Crystallogr. 36, 356–365.
Oaki, Y., 2017. Morphology design of crystalline and polymer materials from nanoscopic to macroscopic scales. Bull. Chem. Soc. Jpn. 90 (11), 776–788.
Pedersen, J.S., Valen, E., Velazquez, A.M.V., Parker, B.J., Rasmussen, M., Lindgreen, S., 2014. Genome-wide nucleosome map and cytosine methylation levels of an ancient human genome. Genome Res. 24 (3), 454–466.
Peer, D., Karp, J.M., Hong, S., Farokhzad, O.C., Margalit, R., Langer, R., 2007. Nanocarriers as an emerging platform for cancer therapy. Nat. Nanotechnol. 2, 751–760.
Policianova, O., Brus, J., Hruby, M., Urbanova, M., Zhigunov, A., Kredatusova, J., Kobera, L., 2014. Structural diversity of solid dispersions of acetylsalicylic acid as seen by Solid-State NMR. Mol. Pharm. 11, 516–530.
Qiu, F., Song, B., Zhong, D.F., 2005. Influence of dosolvent assisted grindinge forms on pharmacokinetics of daidzein and its main metabolite daidzein-7-O-glucuronide in rats. Acta Pharmacol. Sin. 26 (9), 1145–1152.
Rietveld, H.M., 1969. A profile refinement method for nuclear and magnetic structures. J. Appl. Crystallogr. 2, 65–71.
Rivas, M., Garay, R.P., Escanero, J.F., Cia, P., Alda, J.O., 2002. Soy milk lowers blood pressure in men and women with mild to moderate essential hypertension. J. Nutr. 132 (7), 1900–1902.
Sanphui, P., Goud, N.R., Khandavilli, U.B.R., Nangia, A., 2011. Fast dissolving curcumin cocrystals. Cryst. Growth Des. 11, 4135–4145.
Sarkar, A., Rohani, S., 2015. Cocrystals of acyclovir with promising physicochemical properties, pharmaceutics. Drug Deliv. Pharma. Technol. 98–105.
Setchell, K.D., Cassidy, A., 1999. Dietary isoflavones: biological effects and relevance to human health. J. Nutr. 129 (3), 758S–767S.
Setchell, K.D., Brown, N.M., Lydeking-Olsen, E., 2002. The clinical importance of the metabolite equol—a clue to the effectiveness of soy and its isoflavones. J. Nutr. 132 (12), 3577–3584.
Shan, N., Zaworotko, M.J., 2008. The role of cocrystals in pharmaceutical science. Drug Discov. Today 13 (9), 440–446.
Shen, Q., Li, X., Yuan, D., Jia, W., 2010. Enhanced oral bioavailability of daidzein by self-microemulsifying drug delivery system. Chem. Pharm. Bull. 58 (5), 639–643.
Shete, G., Pawar, Y.B., Thanki, K., Jain, S., Bansal, A.K., 2015. Oral bioavailability and pharmacodynamic activity of hesperetin nanocrystals generated using a novel bottom-up technology. Mol. Pharm. 12 (4), 1158–1170.
Smith, A.J., Kavuru, P., Arora, K.K., Kesani, S., Tan, J., Zaworotko, M.J., et al., 2013. Crystal engineering of green tea epigallocatechin-3-gallate (EGCg) cocrystals and pharmacokinetic modulation in rats. Mol. Pharm. 10 (8), 2948–2961.
Sojitra, P., Raval, A., Kothwala, D., Kotadia, H., Adeshara, S., 2010. Covalently conjugation of genistein with biodegradable poly L-lactide. Artif. Organs 20090220, 38.
Sowa, M., Ślepokura, K., Matczak-Jon, E., 2012. A 1: 1 cocrystal of baicalein with nicotinamide. Acta Crystallogr. Sect. C Cryst. Struct. Commun. 68 (7), o262–o265.
Stancanelli, R., Mazzaglia, A., Tommasini, S., Calabrò, M., Villari, V., Guardo, M., et al., 2007. The enhancement of isoflavones water solubility by complexation with modified cyclodextrins: a spectroscopic investigation with implications in the pharmaceutical analysis. J. Pharm. Biomed. Anal. 44 (4), 980–984.
Thakuria, R., 2018. SarmaB.Drug-Drug and drug-nutraceutical cocrystal/salt as alternative medicine for combination therapy: a crystal engineering approach. Crystals 8 (2), 101.
Tikkanen, M.J., Adlercreutz, H., 2000. Dietary soy-derived isoflavone phytoestrogens: could they have a role in coronary heart disease prevention? Biochem. Pharmacol. 60 (1), 1–5.
Ueda, A., 2017. Development of novel functional organic crystals by utilizing proton- and π-electron-donating/accepting abilities. Bull. Chem. Soc. Jpn. 90 (11), 1181–1188.
Wang, H.-Z., Zhang, Y., Xie, L.-P., Yu, X.-Y., Zhang, R.-Q., 2002. Effects of genistein and daidzein on the cell growth, cell cycle, and differentiation of human and murine melanoma cells. J. Nutr. Biochem. 13 (7), 421–426.
Whaley, W.L., Rummel, J.D., Kastrapeli, N., 2006. Interactions of genistein and related isoflavones with lipid micelles. Langmuir 22 (17), 7175–7184.
Xavier, C.R., Silva, A.P.C., Schwingel, L.C., Borghetti, G.S., Koester, L.S., Mayorga, P., et al., 2010. Improvement of genistein content in solid genistein/-cyclodextrin complexes β. Quím. Nova 33 (3), 587–590.
Yadav, A., Shete, A., Dabke, A., Kulkarni, P., Sakhare, S., 2009. Co-crystals: a novel approach to modify physicochemical properties of active pharmaceutical ingredients. Indian J. Pharm. Sci. 71 (4), 359.
Zhang, Z., Huang, Y., Gao, F., Bu, H., Gu, W., Li, Y., 2011. Daidzein–phospholipid complex loaded lipid nanocarriers improved oral absorption: in vitro characteristics and in vivo behavior in rats. Nanoscale 3 (4), 1780–1787.
Zou, J., Shi, W., Wang, J., Bo, J., 2005. Encapsulation and controlled release of a hydrophobic drug using a novel nanoparticle-forming hyperbranched polyester. Macromol. Biosci. 5 (7), 662–668.